Mixed Barrier Model for the Mixed Glass Former Effect in Ion Conducting Glasses

Michael Schuch,[1] Christian R. Müller,[1] Philipp Maass,[1,2,*] and Steve W. Martin[3]

[1]*Institut für Physik, Technische Universität Ilmenau, 98684 Ilmenau, Germany*
[2]*Fachbereich Physik, Universität Osnabrück, Barbarastrasse 7, 49069 Osnabrück, Germany*
[3]*Department of Material Science & Engineering, Iowa State University, Ames, Iowa 500100, USA*

(Received 19 December 2008; published 8 April 2009)

Mixing two types of glass formers in ion conducting glasses can be exploited to lower conductivity activation energy and thereby increasing the ionic conductivity, a phenomenon known as the mixed glass former effect (MGFE). We develop a model for this MGFE, where activation barriers for individual ion jumps get lowered in inhomogeneous environments containing both types of network forming units. Fits of the model to experimental data allow one to estimate the strength of the barrier reduction, and they indicate a spatial clustering of the two types of network formers. The model predicts a time-temperature superposition of conductivity spectra onto a common master curve independent of the mixing ratio.

DOI: 10.1103/PhysRevLett.102.145902 PACS numbers: 66.30.Dn

Ion conducting glasses are attractive electrolyte materials since their composition can be varied to a large extent and hence adapted to specific needs. They can be used in many devices, such as, batteries, electrochromic windows, chemical sensors, and supercapacitors. High ionic conductivities are needed for optimizing glassy electrolytes in these applications and it is important to find methods for enhancing them in a systematic way.

One method for increasing the ionic conductivity is the mixing of different types of glass formers. Considering a glass of general composition $yM_2X + (1-y)[(1-x)A + xB]$ with two network formers A, B and an alkali modifier M_2X (where X is O or S) with fixed mole fraction y, the activation energy $E_\sigma(x)$ of the dc conductivity $\sigma_{\rm dc}(x)$ often passes through a minimum as a function of the mixing ratio x, causing a pronounced maximum in the conductivity. This phenomenon is commonly referred to as the ''mixed glass former effect'' (MGFE) [1]. The MGFE has been found in various glass systems, e.g., SiO_2-B_2O_3 [2], P_2O_5-B_2O_3 [3,4], GeS_2-SiS_2 [5], P_2O_5-TeO_2 [6], TeO_2-B_2O_3 [7], MoO_3-TeO_2 [8], and GeO_2-GeS_2 [9] mixed glass former systems.

Different from the prominent mixed alkali effect [10], the MGFE appears to be less universal. For example, in borosilicates it has been argued that it occurs only in rapidly quenched glasses with high concentration of mobile ions [11] and in the P_2O_5-TeO_2 system more than one minimum in the activation energy has been observed [6]. With respect to a classification of different systems, we distinguish a situation I, where, upon varying x, the local geometry of the units of each of the network formers remains the same (as, e.g., in the GeO_2-GeS_2 system with tetrahedral units) from a situation II, where the coordination number of elementary units of a network former changes (e.g., in borophosphates, the ratio of tetrahedral BO_4 to trigonal BO_3 units).

Because of the mixing of glass formers, the free-energy landscape for the ion migration changes and in general both the energy levels for the residence sites of the mobile ions and the saddle point energies for ion jumps between neighboring sites are affected. In situation II, one can expect that the dominant effect is associated with a change of the site energies, since different local geometries of the network forming units (NFU) are associated with strong variations in the spatial counter-charge distribution. In situation I, in contrast, it can be expected that the dominant effect is associated with reduced barrier energies along jump paths with heterogeneous local environments (i.e., containing different glass forming units) compared to those with homogeneous local environments.

In this Letter, we concentrate on situation I, where a basic modeling should have at least two components: A measure for the strength of the barrier reduction and a prescription of how the fraction of homogeneous to heterogeneous environments and their spatial distribution changes with the mixing ratio x. Based on these minimal ingredients we develop a ''mixed barrier model'' (MBM) and show that a simple realization of this model allows one to fit experimental data and to give an estimate of the strength of the barrier reduction effect. This strength turns out to be only weakly affected by spatial clustering of the two types of network formers. As a universal feature independent of specific model implementations, the MBM predicts a scaling of the ac conductivity with respect to both temperature and mixing ratio x.

The MBM can be considered as a variant of the random barrier model (RBM) [12] with a distribution of activation barriers changing with x. The mobile ions in the glassy network (or mobile charge carriers [13]) perform thermally activated jumps between neighboring sites with rate $\nu \exp(-\mathcal{E}_i/k_BT)$, where ν is an attempt frequency ($\sim 10^{12}$ Hz) and $\mathcal{E}_i$ a microscopic energy barrier, whose mean value is different for different environments of the surrounding NFU. For simplicity we distinguish between a homogeneous environment (A or B), where the surrounding units are all of the same type and a mixed environment

(AB), where both types of units are present. For each of these environments we introduce a smooth distribution $\psi_\alpha(\mathcal{E})$ of barriers ($\alpha = A, AB, B$), with ψ_{AB} having a lower mean than ψ_A and ψ_B to account for reduced barrier energies in heterogeneous environments [14]. If the environments occur randomly along the migration path (subset of all possible transitions) with probabilities $p_\alpha(x)$, the activation energy $E_\sigma(x)$ can be calculated from the critical path analysis of percolation theory [15]: $\int_0^{E_\sigma} d\mathcal{E}\,\psi(\mathcal{E}, x) = p_c$, where $\psi(\mathcal{E}, x) = \sum_\alpha p_\alpha(x)\psi_\alpha(\mathcal{E})$, and p_c is the percolation threshold for the occurrence of a connected path of transitions through the system.

Choosing box distributions with support $0 \le \mathcal{E} \le E_\alpha$ with $E_{AB} < E_A \le E_B$, only the E_α are needed for parameterization, and we obtain (a) for $E_\sigma(x) \le E_{AB} \le E_A$

$$E_\sigma(x) = \frac{p_c}{p_A(x)E_A^{-1} + p_B(x)E_B^{-1} + p_{AB}(x)E_{AB}^{-1}}, \qquad (1)$$

while (b) $E_\sigma(x) = [p_c - p_{AB}(x)][p_A(x)E_A^{-1} + p_B(x)E_B^{-1}]^{-1}$ for $E_{AB} \le E_a(x) \le E_A$, and (c) $E_\sigma(x) = [p_c - p_{AB}(x) - p_A(x)][p_B(x)E_B^{-1}]^{-1}$ for $E_{AB} \le E_A \le E_\sigma(x)$.

Despite the simplicity of this model, Eq. (1) can be used to estimate the strength E_{AB}/E_B of barrier reduction by fitting experimental data. For this fitting we first note that cases (b) and (c) require $E_{AB}/E_B < p_c$, since $E_\sigma(1) = p_c E_B$ gives the maximum of the activation energy. Hence, with percolation thresholds smaller than 0.5 and variations of activation energies not larger than by a factor of 2, the generic situation corresponds to Eq. (1). For the probabilities $p_\alpha(x)$ we make the ansatz $p_A(x) \sim (1-x)^z$ and $p_B(x) \sim x^z$ [$p_{AB}(x) = 1 - p_A(x) - p_B(x)$], where z is a mean number of NFU influencing the local transition barriers. The activation energies of the pure systems are used to determine the ratio $E_A/E_B = E_\sigma(0)/E_\sigma(1)$. Knowing this value, $E_\sigma(x)/E_\sigma(1)$ from Eq. (1) is only a function of E_{AB}/E_B and z (independent of p_c), $E_\sigma(x)/E_a(1) = f(E_{AB}/E_B, z)$, which allows us to determine these remaining two parameters by a least-square fit.

Figure 1 shows such an analysis for the two systems $y\mathrm{Li_2S} + (1-y)[x\mathrm{GeS_2} + (1-x)\mathrm{SiS_2}]$ [5] and $y\mathrm{Li_2S} + (1-y)[x\mathrm{GeO_2} + (1-x)\mathrm{GeS_2}]$ [9]. In view of the scatter in the experimental data, the fitted curves are in fair agreement for parameter values $z \simeq 2$ and a barrier reduction $E_{AB}/E_B \simeq 60\%$. As a further example, we also fit the MGFE found in the rapidly quenched system $(1-x)\mathrm{Li_4SiO_4} + x\mathrm{Li_3BO_3}$, which exhibits no network structure but can be viewed as an ionic glass composed of $\mathrm{SiO_4^{4-}}$ and $\mathrm{BO_3^{3-}}$ anions, and $\mathrm{Li^+}$ cations. Since the Coulomb traps created by the anions are of comparable strength per Li ion, we can also for this system conjecture that the dominant changes of the energy landscape are associated with energy barriers, corresponding to situation I. Again we find a reasonable agreement with the experiment with similar values for z and E_{AB}/E_B.

The value of $z \simeq 2$, which describes the mean number of network forming units influencing the local transition barriers, appears to be rather small. For example, when distributing A and B units randomly among the centers of a cubic lattice, where the mobile charge carriers jump along the lattice bonds, one would have $z = 4$. The small value points to the presence of an effective (renormalized) z when fitting with Eq. (1), which could be caused by spatial correlations between the jump barriers. Indeed, partial phase-separation effects of different network formers are often discussed in the literature. For the $\mathrm{GeO_2}$-$\mathrm{GeS_2}$ system, evidence for spatial correlations was provided recently by reverse Monte Carlo modeling [16], where it was found that the glass structure is built up from independent chains of each of the network formers with the charge carriers occupying the space in between the chains. In the $\mathrm{GeS_2}$-$\mathrm{SiS_2}$ system, small angle x-ray scattering measurements [5] showed clear phase separation tendencies of the two network formers.

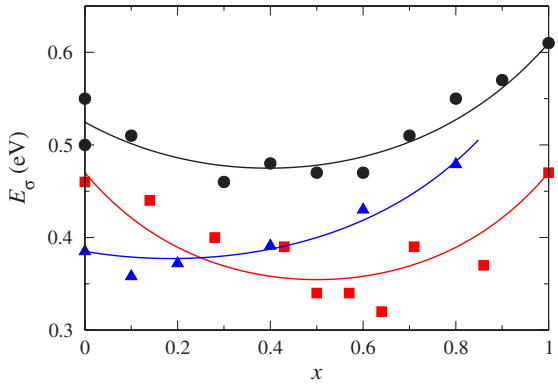

FIG. 1 (color online). Conductivity activation energy for $0.3\mathrm{Li_2S} + 0.7[(1-x)\mathrm{SiS_2} + x\mathrm{GeS_2}]$ (■) [5], $\mathrm{Li_2S} + [(1-x)\mathrm{GeS_2} + x\mathrm{GeO_2}]$ (▲) [9], and rapidly quenched $x\mathrm{Li_4SiO_4} + (1-x)\mathrm{Li_3BO_3}$ (•) [2] glasses. The fits (solid lines) according to Eq. (1) yield $E_{AB}/E_B = 0.69$, $z = 2.8$ for the $\mathrm{SiS_2}$-$\mathrm{GeS_2}$ system and $E_{AB}/E_B = 0.67$, $z = 2.0$ for the $\mathrm{SiO_2}$-$\mathrm{B_2O_3}$ system. Because of the missing value for $x = 1$ in the $\mathrm{GeS_2}$-$\mathrm{GeO_2}$ system, we fixed $z = 2$ and fitted $E_\sigma(x)/E_\sigma(x = 0.8)$, yielding $E_A/E_B = 0.63$ and $E_{AB}/E_B = 0.57$.

In order to study the effect of partial demixing in the MBM, we proceed by investigating the consequences of a kinetically suppressed phase-separation. We presume that during cooling, phase separation sets in above the glass transition temperature T_g, which below T_g freezes in. Inside the resulting domains the pure environments prevail and the barrier reduction occurs in the interfacial regions. Specifically we consider the spinodal decomposition of A and B units with nearest neighbor interactions corresponding to an Ising model at temperature $T = 0.22T_c$. The NFU are placed on the centers of a cubic lattice with random start configuration, and the demixing is carried out by exchanging units A and B according to the Kawasaki exchange dynamics until the characteristic domain size reaches a given value l [17]. Energy barriers are assigned to the lattice bonds with pure (either 4 A or 4 B units) or mixed environments by drawing them from the box distri-

butions considered above with a symmetric choice of parameters $E_A = E_B = 2E_{AB}$.

Again we can determine the activation energy from a critical path analysis, but the equation $\int_0^{E_\sigma} d\mathcal{E}\,\psi(\mathcal{E}, x) = p_c$ can no longer be used since it applies only to a random distribution of the barriers. We calculated E_σ directly from the disorder configurations by determining the critical barrier that a charge carrier needs to surmount in order to move through the system.

In addition we calculated the frequency-dependent conductivity $\sigma(\omega, T)$ by the velocity autocorrelation method [18]. Using these spectra (cf. Fig. 3), we can determine E_σ from Arrhenius plots of the low-frequency limit $\sigma_{\rm dc}(T)$. As shown for representative examples in the inset of Fig. 2, the slopes of the lines in the Arrhenius plot are in excellent agreement with the E_σ values calculated from the critical path analysis.

The dependence of the function $E_\sigma(x)$ on the domain size l (in units of the lattice spacing a) is displayed in Fig. 2. For small $l \lesssim 2.3$, the behavior is almost indistinguishable from a random barrier distribution, corresponding to E_σ from Eq. (1) with $z = 4$ (solid line). For larger l the curves $E_\sigma(x)$ flatten and the MGFE becomes weaker. We find that these curves for larger l can still be well described by Eq. (1), if we use an effective z value (dashed lines). The effective z decreases with l, and for $l = 6.2$ reaches $z = 2.6$. This value is comparable to those found from the analysis of the experimental data in Fig. 1. The agreement with Eq. (1) moreover demonstrates that we would obtain barrier reductions close to the exact one ($E_{AB} = 0.5E_B$), if we fitted the curves for larger l as in Fig. 1. This gives some confidence in the above estimate of the barrier reduction effect.

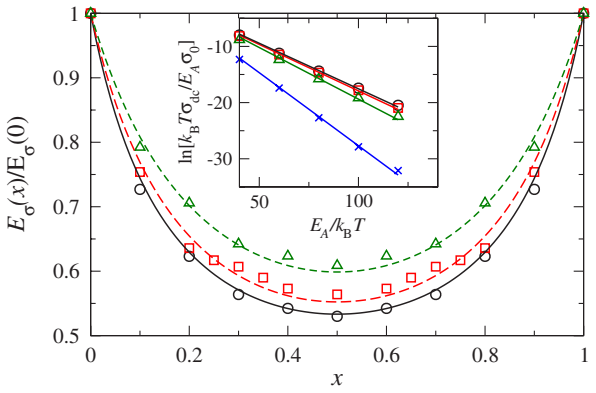

FIG. 2 (color online). Normalized activation energy $E_\sigma(x)/E_\sigma(0)$ for different domain sizes $l = 2.4$ (○), 4.3 (□), and 6.2 (△). The solid line marks the solution Eq. (1) with $z = 4$, and the dashed lines are fits to Eq. (1) with z as fitting parameter ($E_{AB}/E_B = 0.5$ fixed). Inset: Arrhenius plots of the conductivity (in units of σ_0, cf. caption of Fig. 3) calculated by using the velocity autocorrelation method [18] for $x = 0.0$ (×), and for $x = 0.4$ with $l = 2.4$ (○), 4.3 (□), and 6.2 (△); lines are least-square fits.

It is clear that the MBM is a simple approach, but it does allow us to see how barrier reduction in inhomogeneous environments leads to the MGFE and how large the strength of this reduction might be expected to be. For a more microscopic description one would need to incorporate detailed structural information specific for the glass system under consideration.

On the other hand, we can ask if there exist universal features of the ion transport behavior independent of microscopic details. For a given ion conducting glass composition, a universal feature is the time-temperature (or frequency-temperature) scaling of conductivity spectra [12]. This scaling means that conductivity spectra at different temperatures fall onto a common master curve, if one divides $\sigma(\omega, T)$ by $\sigma_{\rm dc}$ and ω by $\omega_c(T)$, where $\omega_c(T)$ is the crossover frequency to the dispersive regime, as determined, e.g., by the condition $\sigma(\omega_c(T), T) = 2\sigma_{\rm dc}$. The question arises whether this scaling can be extended so that spectra of different glass compositions collapse onto a

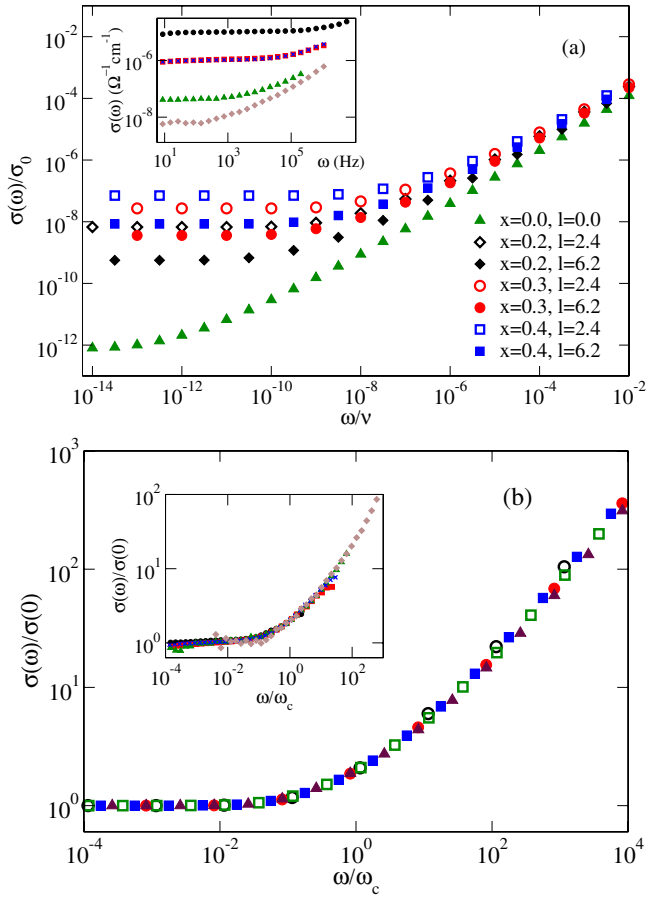

FIG. 3 (color online). (a) Conductivity spectra $\sigma(\omega)$ (in units of $\sigma_0 = ne^2\nu a^2/E_A$ with n the number concentration of mobile ions) for fixed temperature, $k_B T/E_A = 0.01$, two domain sizes l, and various mixing ratios x. Inset: Conductivity spectra of $LiS_2 + (1 - x)GeS_2 + xGeO_2$ glasses for $x = 0.1$ (●), $x = 0.2$ (×), and $x = 0.4$ (■) at $T = 253$ K, as well as for $x = 0.6$, $T = 224$ K (▲), and $x = 0.8$, $T = 231$ K (◆). (b) Scaled conductivity spectra for the data shown in (a).

common curve. For variations of the modifier content (mobile ion concentration) such ''superscaling'' has been observed approximately [19], while deviations from superscaling have been found when mixing different types of mobile ions [20].

In the following we investigate what behavior can be expected for the MGFE based on the MBM. In the limit of $l \rightarrow 0$, superscaling is expected, since it was shown in the RBM that time-temperature scaling is independent of the form of the barrier distribution [12]. Indeed, we have confirmed this expectation by our simulations for the differing distributions with varying x. So far, however, it has not been investigated, whether the scaling remains valid in the presence of spatial correlations of the barriers, as they occur in the course of the partial phase separation discussed above. Indeed we find a superscaling with respect to variations of both x and l. This is shown in Fig. 3, where various conductivity spectra for different x and l in panel (a) are superimposed onto a common master curve in panel (b). In the insets of Figs. 3(a) and 3(b) we show corresponding unscaled and scaled conductivity data for the $Li_2S + [(1 - x)GeS_2 + xGeO_2]$ system. The collapse of these data in Fig. 3(b) nicely supports the prediction of superscaling by the MBM. It is noted that the spectra in Fig. 3(a) also show that the MGFE becomes weaker for higher frequencies, as expected for an ion dynamics governed by lower barriers with decreasing length scale (or increasing frequency) [21].

In summary a model for the MGFE has been developed, which is based on a reduction of jump barriers for the mobile charge carriers in local environments containing different types of NFU. This model has been applied to glasses with the same local geometry of the two types of NFU upon mixing. The model is able to fit experimental data for the conductivity activation energy for representative systems and thus allows one to estimate the strength of the barrier reduction effect. It was shown how a kinetically frozen phase separation influences the MGFE and can be effectively described by a renormalized coordination in the environments of the jump paths, in agreement with values obtained from the fits. The MBM predicts a time-temperature superposition of conductivity spectra onto a common master curve independent of the mixing ratio x. This prediction could be confirmed by data available for one glass system and should be tested for other glass compositions in the future. From the theoretical perspective, it would be important to critically test the underlying model assumptions by calculations on the molecular level as, e.g., electronic structure calculations of representative clusters and molecular dynamics simulations.

We would like to thank V. Petkov for very valuable discussions. Work on this project was supported in the Materials World Network by the Deutsche Forschungsgemeinschaft (DFG Grant No. MA 1636/3-1) and by the NSF (NSF DMR Grant No. 0710564).

*philipp.maass@uni-osnabrueck.de; http://www.tu-ilmenau.de/theophys2

[1] M. D. Ingram, Phys. Chem. Glasses **28**, 215 (1987).
[2] M. Tatsumisago, N. Machida, and T. Minami, J. Ceram. Soc. Jpn. (Jpn. Ed., 1950-1987) **95**, 197 (1987).
[3] D. Zielniok, C. Cramer, and H. Eckert, Chem. Mater. **19**, 3162 (2007); D. Zielniok, H. Eckert, and C. Cramer, Phys. Rev. Lett. **100**, 035901 (2008).
[4] P. S. Anantha and K. Hariharan, Mater. Chem. Phys. **89**, 428 (2005).
[5] A. Pradel, N. Kuwata, and M. Ribes, J. Phys. Condens. Matter **15**, S1561 (2003).
[6] D. Coppo, M. J. Duclot, and J. L. Souquet, Solid State Ionics **90**, 111 (1996).
[7] B. V. R. Chowdari and P. P. Kumari, Solid State Ionics **86–88**, 521 (1996).
[8] B. V. R. Chowdari and P. P. Kumari, J. Phys. Chem. Solids **58**, 515 (1997).
[9] Y. Kim, J. Saienga, and S. W. Martin, J. Phys. Chem. B **110**, 16 318 (2006); Y. Kim and S. W. Martin, Solid State Ionics **177**, 2881 (2006).
[10] D. E. Day, J. Non-Cryst. Solids **21**, 343 (1976).
[11] L. F. Maia and A. C. M. Rodrigues, Solid State Ionics **168**, 87 (2004).
[12] J. C. Dyre and T. B. Schrøder, Rev. Mod. Phys. **72**, 873 (2000).
[13] Molecular dynamics simulations and general theoretical considerations suggest that only a relatively small fraction of about 10% of the ionic residence sites are empty at any given time. This gives reason to consider the vacancies as the mobile charge carriers.
[14] In first approximation, the Coulomb interaction between the mobile ions can be considered to be included in these distributions as a constant contribution, since the total mobile ion concentration is almost independent of x.
[15] S. Tyč and B. I. Halperin, Phys. Rev. B **39**, 877 (1989).
[16] D. Le Messurier, V. Petkov, S. W. Martin, Y. Kim, and Y. Ren, J. Non-Cryst. Solids (to be published).
[17] For details of the Kawasaki dynamics, see D. P. Landau and K. Binder, *A guide to Monte Carlo Simulations in Statistical Physics* (Cambridge University Press, Cambridge, England, 2005), p. 115. The domain size l characterizes the extent of regions with A and B excess. It is the same here for both components and determined by taking the first zero in the AA (or BB) correlation function.
[18] T. B. Schrøder, Europhys. Lett. **81**, 30 002 (2008).
[19] B. Roling, A. Happe, K. Funke, and M. D. Ingram, Phys. Rev. Lett. **78**, 2160 (1997); B. Roling, Solid State Ionics **105**, 185 (1998); D. L. Sidebottom, Phys. Rev. Lett. **82**, 3653 (1999).
[20] J. Zhang and D. L. Sidebottom, J. Non-Cryst. Solids **288**, 18 (2001).
[21] J. C. Dyre, P. Maass, B. Roling, and D. Sidebottom, Rep. Prog. Phys. **72**, 046501 (2009).